29th EPS Conference on Plasma Phys. and Contr. Fusion Montreux, 17-21 June 2002 ECA Vol. **26B**, O-5.06 (2002)

STUDY OF ELMs ON ASDEX UPGRADE USING REFLECTOMETRY MEASUREMENTS WITH HIGH TEMPORAL AND SPATIAL RESOLUTION

I.Nunes[1], G.D.Conway[2], M.Manso[1], M.Maraschek[2], F.Serra [1], W.Suttrop[2] and the CFN[1] and ASDEX Upgrade[2] Teams

[1] *Centro de Fusão Nuclear, Associação Euratom-IST, Lisboa, Portugal*

[2] *Max-Planck Institut fuer Plasmaphysik, EURATOM-Association IPP, Garching D-85748, Germany*

1. Introduction

The impact of ELM activity on the edge plasma in ASDEX Upgrade tokamak discharges are assessed using high resolution (time and spatial) measurements from microwave reflectometry. The dynamics of type I and type III ELMs is resolved with broadband fast-swept (25 μs and 50 μs) profile reflectometry and tunable frequency multichannel fluctuation reflectometry with high time and spatial resolution [1]. The broadband density profile reflectometry system consists of eight O-mode channels probing simultaneously the high field (HFS) and low field sides (LFS) at the midplane over the density range [0.30-6.64] $\times 10^{19}$ m^{-3}. The typical sweep rate is 25 μs (35 μs repetition period) with 3066 profiles per shot. The fluctuation system has two O-mode channels on the LFS (35 to 72 GHz) with a 1 or 2 μs sample rate and 4.2 MS of data per channel.

2. Type I ELM characterization

Three phases of the ELM are identified: precursor phase, MHD phase and recovery phase. Because of their lower frequency and higher impact on the profiles, type-I ELMs provide a clearer picture of the three phases. In this section each phase for the type I ELM is characterized in terms of changes in the reflectometry data.

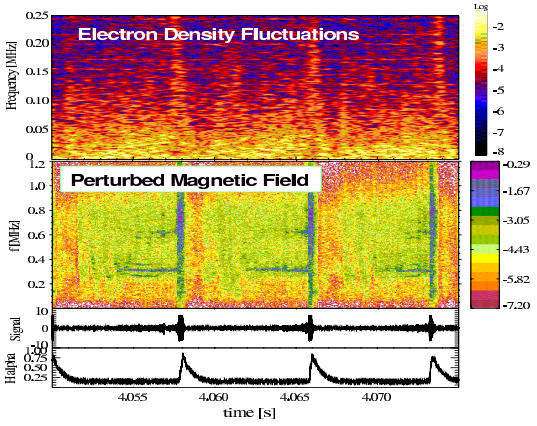

Figure 1: *Spectrogram of reflectometer signal fluctuation ($n_e = 2.98 \times 10^{19} m^{-3}$) and fast Rogowski coil*

2.1 Precursor Phase Figure 1 shows two spectrograms: (a) of magnetic pick-up coil fluctuations and (b) from a fixed frequency reflectometer channel (probing a density of 2.98×10^{19}m^{-3}) for AUG shot #14532. This is a 1.0 MA/2.0 T standard H-mode with a $q_{95} = 3.23$ and low triangularity $\delta \sim 0.15$. The sweep rate is 50 μs for this discharge. The magnetic measurements show a clear precursor at ~400 kHz [2], The reflectometer measurements are restricted to 250 kHz and do not show the precursor effect. The reflectometer measurements nevertheless do show an increase of broadband fluctuations prior to the ELM onset, this was also observed in

JET [3]. The effect of the precursor is tracked in the high resolution profile measurements, by an increase in low frequency perturbations of the profile in the scrape-off layer (SOL), (figure 2). The profile perturbation starts a few milliseconds ($\sim 1-2$) before the onset of the ELM and is seen on both the HFS and LFS.

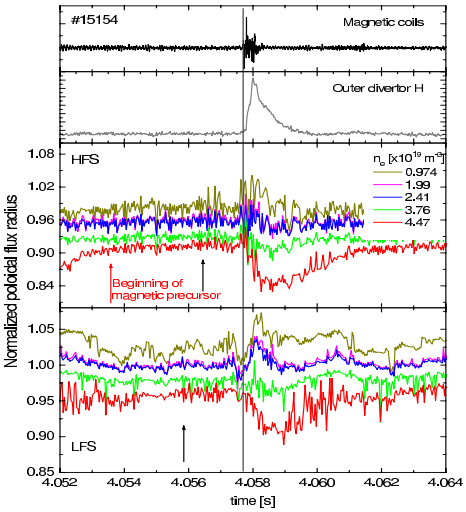

Figure 2: *Radial movement HFS and LFS cutoff layers as function of time for several densities*

2.2 MHD Phase The distance from the reflectometer antenna to the cutoff layer $R(F)$ is calculated from the measured group delay $\tau_g(F)$ as a function of microwave probing frequency F from:

$$R(F) \propto \int \tau_g(f) \frac{df}{\sqrt{F^2 - f^2}}.$$

In broadband swept measurements the location of the cut-off layer R(F) is obtained from the measured group delay τ_g as a function of microwave probing frequency. This gives directly (O-mode) the density at the cut-off layer, accordingly to: $n_e \sim (F/9)^2$. Figure 3 shows two spectrograms of the reflected signal obtained with a sliding FFT, for shot #14532. As the spectrograms give the time resolved beat frequency (interference between incident and reflected waves), the group delay curves can be visualised directly. Between ELMs (figure 3a) a clear τ_g characteristic is obtained indicating a quiescent density profile, whereas during the MHD phase (figure 3) the $\tau_g(F)$ line is destroyed due to the plasma density perturbations.These clear signal perturbations lasts $\sim$200 μs and coincides with the time interval where enhanced magnetic perturbations occur (top trace in figure 3). A comparison of the HFS and LFS data gives a delay of $\sim$50 - 70 μs in the onset of the HFS profile distortion relative to LFS. This observation is consistent with the expected ballooning character of the mode.

2.3 Recovery Phase Imediately after the chaotic phase ($\sim$200μs) - where it is not possible to reliably reconstruct the electron density profiles - the first reliable profile (shown in figure 4) displays a decrease in the edge density gradient with the pedestal density collapsing and the SOL density increasing. As the ELM recovery phase proceeds the density profile rotates about a pivot point to resume its original shape. This pivot point is approximately at half the pedestal density and radially close to the separatrix. Outside the pivot point the SOL density is quickly lost and the profile recovers its initial gradient in $\sim$3-4 ms. However, inside the pivot point the density profile recovery is much longer ($\sim$tens of ms) and, depending of the ELM frequency, may not fully recover its former shape before the next ELM event. The density profile affected area by the ELM (inside the pivot point) is $\sim$14 cm wide.

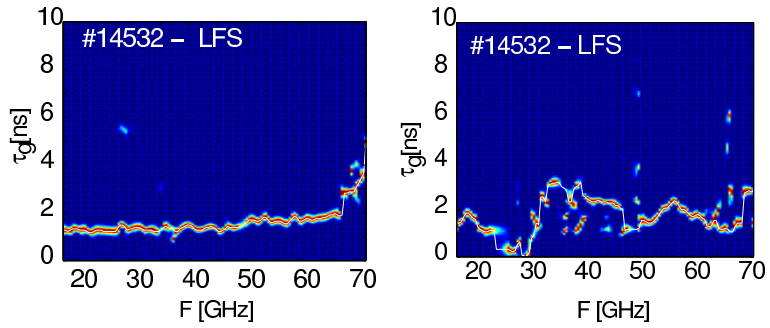

Figure 3: *Reflectometry group delay a) before the ELM and b) during the MHD phase of the ELM*

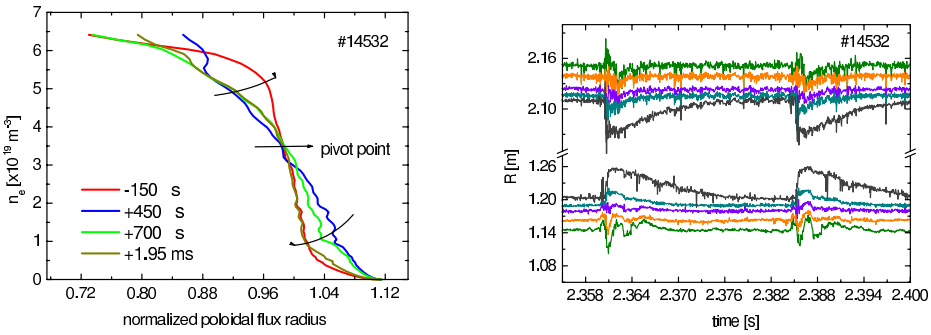

Figure 4: *(a) Density profile evolution during recovery phase and (b) time traces for specific density cut-off layers. Times in figure (a) are with respect to the onset of the ELM*

3. Type III ELMs

Due to the higher frequency of type-III ELMs, the definition of the three phases is not so clear. However some conclusions can nevertheless be drawn. Figure 5 shows the radial displacement for selected cutoff layers in a 0.8 MA/2.3 T type-III ELM discharge #15773 with an ELM frequency of 1.8 kHz. For this shot $q_{95} = 4.64$ with triangularity $\delta = 0.15$. The LFS shows a much higher profile perturbation than the HFS. The radial displacement of the cutoff layers due to each ELM can clearly be perceived at the lower densities. The recovery phase shows the same characteristic movement as for type-I ELMs. However, the range of densities where the behaviour of the cutoff layer is consistent with the D_α signal is much narrower than for type-I ELMs. From this the density profile affected area is determined as ~5 cm (measured at HFS).

4 Conclusions

From the type-I ELM comparison at HFS and LFS it was observed that the HFS is less perturbed that the LFS. The precursor phase and MHD phase show a time delay

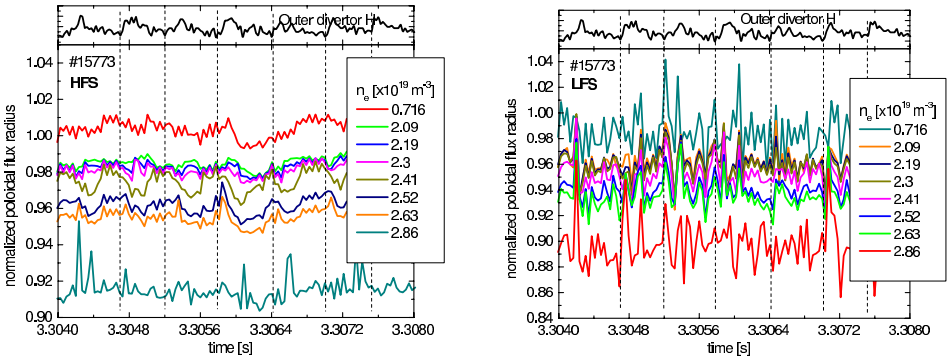

Figure 5: *Radial displacement of density cut-off layers for type-III ELMs at HFS and LFS. LFS shows a much stronger perturbation than HFS*

for the HFS relatively to the LFS consistent with a ballooning character for the ELM. Although the precursor phase and MHD phase show a delay between HFS and LFS, at the recovery phase the behaviour of the profile is symmetric. For type-III ELMs the width of the density profile affected area is ∼5 cm much less compared to ∼14 cm for type I ELMs. Integrating the density profile over the ELM affected enclosed volume before and after the ELM, the particle losses due to the ELM can be determined. For type-I ELMs the average particle loss is $\sim$ 10% of the total pedestal particle content ($n_{e,ped} \times Vplasma$), while for type-III ELMs this value is $\sim$ 5%. The total particle outflux is $\Delta N \times f_{ELM}$. Although the particle losses due to an individual ELM are less for type-III ELMs, the overall particle outflux is larger than for type-I due to the higher ELM frequency.

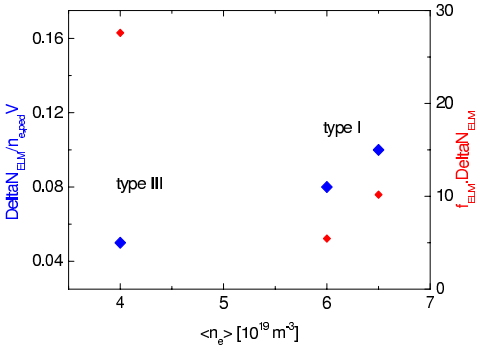

Figure 6: *Particle losses for type-I ($f_{ELM} = 140Hz$)and type-III ELMs ($f_{ELM} = 1.8kHz$) (blue) and particle outflux (red)*

Acknowledgments: The first author would like to thank A. Loarte, G. Saibene and J. Stober for fruitful discussions and comments.

[1] A.Silva *et al*, Rev. Sci. Instrum. **67**, 4138 (1996) [2] T.Bolzonella *et al*, 29^{th} EPS Conf. on Controll. Fusion and Plasma Phys. (Montreux), Switzerland [3] G.D.Conway, JET 1999 [4] P.Varela et al. Rev. Sci. Instrum. **70**, 1060 (1999)